

# Escaping Electron Measurement in Laser-Solid Interactions on Vulcan Target Area West

Contact: yihang.zhang@stfc.ac.uk

## Y. Zhang

Central Laser Facility,  
STFC Rutherford Appleton Laboratory,  
OX11 0QX, United Kingdom

Institute of Physics,  
Chinese Academy of Sciences,  
Beijing 100190, China

## D. Neely

Central Laser Facility,  
STFC Rutherford Appleton Laboratory,  
OX11 0QX, United Kingdom

## G. Scott

Central Laser Facility,  
STFC Rutherford Appleton Laboratory,  
OX11 0QX, United Kingdom

## C. Armstrong

Central Laser Facility,  
STFC Rutherford Appleton Laboratory,  
OX11 0QX, United Kingdom

Department of Physics SUPA  
University of Strathclyde  
Glasgow G4 0NG, UK

## Y. Li

Institute of Physics,  
Chinese Academy of Sciences,  
Beijing 100190, China

## G. Liao

Central Laser Facility,  
STFC Rutherford Appleton Laboratory,  
OX11 0QX, United Kingdom

## H. Liu

Institute of Physics,  
Chinese Academy of Sciences,  
Beijing 100190, China

## D. Rusby

Central Laser Facility,  
STFC Rutherford Appleton Laboratory,  
OX11 0QX, United Kingdom

## P. Brummitt

Central Laser Facility,  
STFC Rutherford Appleton Laboratory,  
OX11 0QX, United Kingdom

## Abstract

An electron spectrometer has been employed in measuring escaping electrons from laser-solid interactions. Electron spectra have been obtained in different laser pulse conditions. Dependence of escaping electron numbers and temperature on the pulse energy, intensity and duration is shown in this report.

## 1 Introduction

Studies of fast electrons generated from a solid target driven by an ultra-intense laser pulse ( $> 10^{18}$  W/cm<sup>2</sup>) are important to understand the physics in laser-plasma interaction physics[1–3]. Electrons are heated by the laser field under various mechanisms such as resonant absorption[4], vacuum heating[5] and  $\mathbf{J} \times \mathbf{B}$  heating[6]. When the forward accelerated electrons reach the target rear surface, a sheath field is established, which impedes the escaping of the electrons, while accelerates ions[7]. The electron dynamics is also related to radiation gener-

ation with a broad spectrum from microwave to gamma-rays[3, 8, 9]. The diagnosis of electrons can help to understand the efficiency and mechanisms of laser absorption and the electron transport in the target, which also enable characterization of subsequent physical processes.

In this report, we measured energy and numbers of escaping electrons from laser-solid interactions with different laser pulse parameters of pulse energy, defocusing and duration.

## 2 Experiment and results

The experiment was carried out at the Vulcan Target Area West (TAW) laser facility. A high intensity laser pulse ( $> 1.4$  ps pulse length) was focused on a 100  $\mu\text{m}$  Cu foil target by an f/3 off-axis parabola (OAP) with a focal spot larger than 5  $\mu\text{m}$ . The incidence angle of the pulse was 30° to the target normal. For the maximum laser energy of 70 J, the highest intensity is  $5 \times 10^{19}$  W/cm<sup>2</sup>. An electron spectrometer (ES) was set at the target rear

side in the forward laser direction, with a distance of 1 m from the target. There was an entrance slit of 1 mm wide at the front side of the ES. Parallel magnets were 17 mm away from the slit, with a length of 25 mm and a magnetic field strength of 0.2 T. A 2 mm thick Al window was set 90 mm away from the magnets, connecting the vacuum chamber and the air. The window blocked electrons with energy below 0.7 MeV. Behind the Al window, a pre-calibrated BAS-SR type image plate (IP)[10] was used to record the electron signal.

Figure 1 (a) shows a recorded signal on the IP. There is an imaging of the slit by X-Rays generated from internal hot electrons, which is usually called the 0<sup>th</sup> order. The escaping electrons were dispersed by the magnetic field. Electrons with higher energy were nearer to the 0<sup>th</sup> order. Figure 1(b) shows a typical electron energy spectrum (green line). Electron numbers are normalized by energy resolution of the ES. The spectrum indicates a quasi-Boltzmann distribution of electrons escaping from a solid target, with temperature of 3.7 MeV.

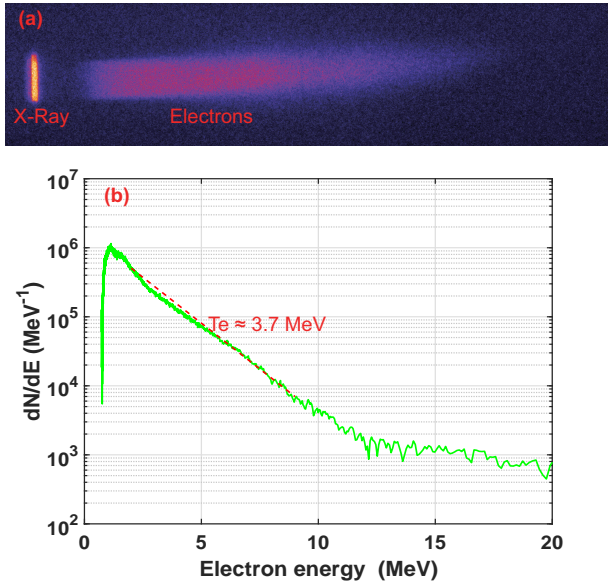


Figure 1: Typical results of electron signal on a IP (a) and the relevant spectrum of a quasi-Boltzmann distribution with temperature of 3.7 MeV (b).

Figure 2 shows energy spectral integrated electron numbers ( $N_e$  in black) and temperature ( $T_e$  in red) for different on-target pulse energy between 14 and 70 J. The correlation between  $N_e$  (and  $T_e$ ) and the driving pulse energy shows a rough monotonically increasing trend. However, the conversion efficiency dose not peak at the maximum pulse energy but at around 48 J.

The effects of laser focusing and relevant intensity on escaping electrons can be seen by Fig. 3(a) and (b) respectively. Electron numbers are normalized to pulse energy. There was a shift from the position of best focusing for both electron numbers and temperature. The peak of the electron temperature appears in a range around

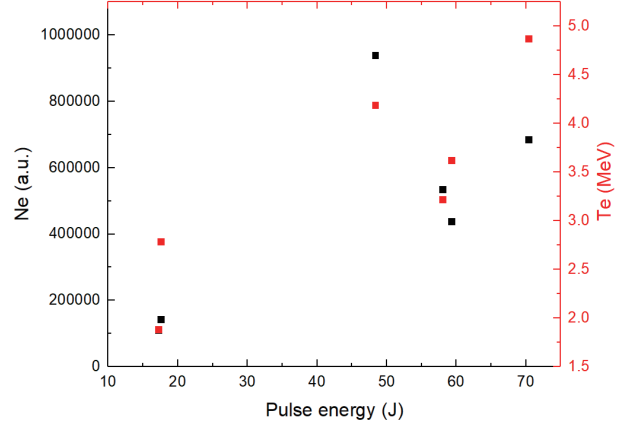


Figure 2: Electron number ( $N_e$  in black) and temperature ( $T_e$  in red) versus on-target laser energy detected by the ES.

40  $\mu\text{m}$  defocusing towards the OAP (-40  $\mu\text{m}$ ), while the electron number peaks at -150 and 80  $\mu\text{m}$ , almost symmetric to -40  $\mu\text{m}$ . The observed asymmetry of electron temperature about the location of best focus may due to the differences in the laser intensity distributions on both sides of best focus for the imperfect laser beam. As the equivalent laser intensity goes lower, the electron temperature decreases correspondingly. The defocusing dependence of the electron number can be understood qualitatively as follows. With pulse defocusing, the number of escaping electrons increases firstly and then decreases. This may arise from the combined actions of three competing effects: the decrease of laser intensity, the increase of electron generation area, and the weakened sheath fields allowing more electrons to escape from the target. Similar dependence on the laser defocusing distance have been observed previously for X-Rays and proton fluxes[11].

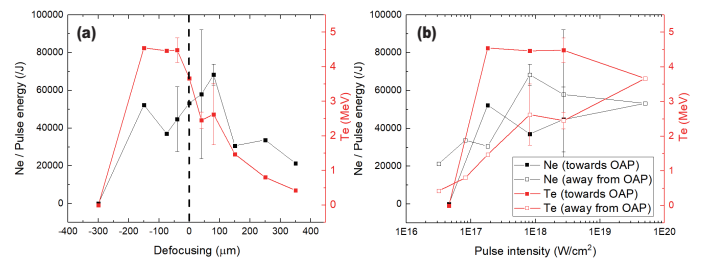


Figure 3: Electron number ( $N_e$  in black) and temperature ( $T_e$  in red) against defocusing distance (a) and relevant pulse intensity (b), respectively. The dash line indicates the position of best focusing.

The dependence of escaping electron numbers and temperature on the pulse duration and relevant intensity is shown in Fig. 3(a) and (b) respectively. The pulse duration is increased gradually to a maximum value of

23 ps. The results indicate both the electron number and energy decrease at longer pulse, except for the case of 1.4 ps ( $1.1 \times 10^{19} \text{ W/cm}^2$ ) due to low pulse energy of 13 J and less electron heating time.

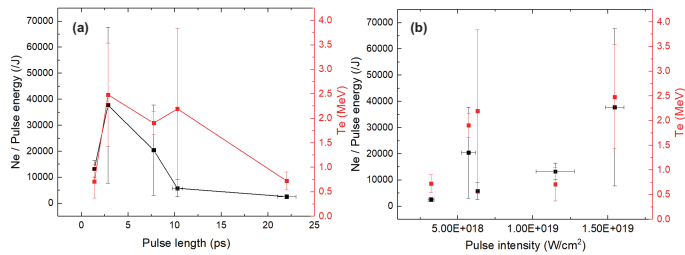


Figure 4: Electron number ( $N_e$  in black) and temperature ( $T_e$  in red) against pulse duration (a) and relevant pulse intensity (b), respectively.

### 3 Conclusion

Escaping electron spectra in intense laser and solid interactions have been measured experimentally. Effects of laser parameters of pulse energy, defocusing and duration on electron numbers and temperature have been observed. The results indicate the variation of energy conversion efficiency when pulse energy increases. Furthermore, escaping electrons are affected by combined actions of the laser intensity, area and time scale for electron generation and sheath field strength for electrons escaping. These results can help as a reference of fast electron adjusting and controlling, to modulate the following ion and radiation sources effected or generated by electrons.

### References

- [1] A. Bell and R. Kingham, “Resistive collimation of electron beams in laser-produced plasmas,” *Physical review letters*, vol. 91, no. 3, p. 035003, 2003.
- [2] Y. Li, X. Yuan, M. Xu, Z. Zheng, Z. Sheng, M. Chen, Y. Ma, W. Liang, Q. Yu, Y. Zhang, *et al.*, “Observation of a fast electron beam emitted along the surface of a target irradiated by intense femtosecond laser pulses,” *Physical review letters*, vol. 96, no. 16, p. 165003, 2006.
- [3] Z.-M. Sheng, Y. Sentoku, K. Mima, J. Zhang, W. Yu, and J. Meyer-ter Vehn, “Angular distributions of fast electrons, ions, and bremsstrahlung x/ $\gamma$ -rays in intense laser interaction with solid targets,” *Physical review letters*, vol. 85, no. 25, p. 5340, 2000.
- [4] P. Gibbon and A. Bell, “Collisionless absorption in sharp-edged plasmas,” *Physical review letters*, vol. 68, no. 10, p. 1535, 1992.
- [5] F. Brunel, “Not-so-resonant, resonant absorption,” *Physical Review Letters*, vol. 59, no. 1, p. 52, 1987.
- [6] S. Wilks, W. Kruer, M. Tabak, and A. Langdon, “Absorption of ultra-intense laser pulses,” *Physical review letters*, vol. 69, no. 9, p. 1383, 1992.
- [7] S. Wilks, A. Langdon, T. Cowan, M. Roth, M. Singh, S. Hatchett, M. Key, D. Pennington, A. MacKinnon, and R. Snavely, “Energetic proton generation in ultra-intense laser–solid interactions,” *Physics of plasmas*, vol. 8, no. 2, pp. 542–549, 2001.
- [8] P. Bradford, N. Woolsey, G. Scott, G. Liao, H. Liu, Y. Zhang, B. Zhu, C. Armstrong, S. Astbury, C. Brenner, *et al.*, “Emp control and characterization on high-power laser systems,” *High Power Laser Science and Engineering*, vol. 6, 2018.
- [9] G.-Q. Liao, Y.-T. Li, Y.-H. Zhang, H. Liu, X.-L. Ge, S. Yang, W.-Q. Wei, X.-H. Yuan, Y.-Q. Deng, B.-J. Zhu, *et al.*, “Demonstration of coherent terahertz transition radiation from relativistic laser-solid interactions,” *Physical review letters*, vol. 116, no. 20, p. 205003, 2016.
- [10] I. Paterson, R. Clarke, N. Woolsey, and G. Gregori, “Image plate response for conditions relevant to laser–plasma interaction experiments,” *Measurement Science and Technology*, vol. 19, no. 9, p. 095301, 2008.
- [11] J. Green, D. Carroll, C. Brenner, B. Dromey, P. Foster, S. Kar, Y. Li, K. Markey, P. McKenna, D. Neely, *et al.*, “Enhanced proton flux in the mev range by defocused laser irradiation,” *New Journal of Physics*, vol. 12, no. 8, p. 085012, 2010.